Once again assumption 2 (i.e., $dC_P/dJ < 0$) guarantees that $dn/dV > 0$. Therefore, if V decreases (at constant throttle), then so must n. If on the contrary the pilot dives (again leaving the throttle alone), the engine speeds up. Equation (8), along with knowledge of $C_P(J)$ for values of J in the vicinity of the initial cruise condition, allows one to proceed stepwise to determine $n(V)$.

One Last Question

But why, one might reasonably ask, is the derivative of the power coefficient with respect to advance ratio always negative? In fact, if no restriction is placed on its domain of definition, it's not true that that derivative is always negative; for examples showing $dC_P/dJ > 0$, see the classic paper of Hartman and Biermann.[3] But it is true that within the fairly well-defined working range of advance ratio values, dC_P/dJ is indeed negative. Why?

The blade element theory of propeller action provides a hodgepodge of contributing conditions, but no direct and simple answer. Or at least this author hasn't found one. Employing the representative blade element analysis of von Mises,[4] however, a satisfactory solution is readily obtained. Von Mises argues that the power coefficient function is of the form

$$C_P = \lambda^2 \mu k \sin \beta'(J_2 - J) \tag{9}$$

where $\lambda \equiv \pi x$, μ is a solidity factor, β' is the blade setting angle (of the representative element at relative station x) with respect to the zero-lift direction, and J_2 is the value of advance ratio at which C_P goes negative. Since all of the numbers in Eq. (9) are positive, dC_P/dJ is negative.

Conclusions

Even in this advanced digital age, classical analytic reasoning can, on occasion, be parsimonious, instructive, and effective. But it seldom does the whole job.

References

[1]Weick, F. E., *Aircraft Propeller Design*, McGraw-Hill, New York, 1930, p. 161.

[2]Kaplan, W., *Advanced Calculus*, Addison-Wesley, Reading, MA, 1952, Chap. 2.

[3]Hartman, E. P., and Biermann, D., "The Aerodynamic Characteristics of Full-Scale Propellers Having 2, 3, and 4 Blades of Clark Y and R.A.F. 6 Airfoil Sections," NACA TR-640, 1938, Fig. 18.

[4]Von Mises, R., *Theory of Flight*, Dover, New York, 1959, p. 308.

Lifting-Line Theory of an Arched Wing in Asymmetric Flight

Gil Iosilevskii*

Technion—Israel Institute of Technology, Haifa 32000, Israel

Introduction

PRANDTL'S lifting-line theory[1,2] is, perhaps, the simplest among aerodynamic theories of high-AR wings in incompressible steady flows. At the essence of the theory, the wing is reduced to a line vortex of variable circulation located at its quarter-chord line; the wake behind the wing is reduced to a continua of noninteracting rectilinear trailing vortices, originating at the quarter-chord and extending to infinity. The equation governing the circulation of the quarter-chord vortex is obtained from the requirement that its local lift should be equal to that calculated from the effective angle of attack (AOA) of the respective wing section.

A recently developed asymptotic theory of high-AR arched wings[3] suggests that if the wing sweep is small enough, Prandtl's lifting-line theory can be extended so as to apply for arched (nonplanar) wings. Toward this end, the wing should be modeled by a planar arched vortex situated perpendicular to the direction in which the wake extends, regardless of the actual wing planform and its orientation relative to the flow. The (infinite) velocity induced by such a vortex on itself should be disregarded, both in constructing the equation governing the circulation of the wing vortex, and in computing the lift and drag forces acting on the wing.

This Note elucidates the extension of the classical lifting line theory for an arched wing of a typical gliding parachute.

Received Jan. 21, 1996; revision received March 20, 1996; accepted for publication April 3, 1996.

*Lecturer, Faculty of Aerospace Engineering.

Lifting-Line Formulation for an Arched Wing

Consider a parachute wing in a steady translatory motion through an (otherwise quiescent) incompressible fluid. Let u and ρ be the velocity of the wing and the density of the fluid, respectively. Consistent with the present design trends, the wing will be assumed to be unswept. It will be also assumed that in the front view the wing can be approximated by an arc of radius R and angle $2\phi_0$ (Fig. 1).

Let C be a right-handed Cartesian coordinate system, selected in such a way that its x axis coincides with the direction of the wing's motion, and the z axis points downward, perpendicular to the line connecting the left and right tips of the wing. Relative to C, the wing and its wake will be modeled by a curved line vortex in the (yz) plane, and by a cylindrical vortex sheet formed on the wing vortex and extending to infinity in the negative x direction. For the sake of being specific, it will be assumed henceforth that the x axis of C passes through the center of the wing's arc.

Let Γ, c, a, $\alpha_\perp$, and α_i, each defined on $(-\phi_0, \phi_0)$, be the sectional circulation, chord length, lift-slope coefficient, geometrical AOA, and induced AOA, respectively; $\alpha_\perp$ and α_i are shown in Fig. 1. By following the same arguments as those of the classical lifting-line theory, the circulation of the model wing is required to be such that its lift $\rho u \Gamma$ equals the lift $\frac{1}{2}\rho u^2 c a(\alpha_\perp - \alpha_i)$ of the actual wing; namely, for each ϕ in $(-\phi_0, \phi_0)$,

$$\Gamma(\phi) = \tfrac{1}{2} u c(\phi) a(\phi)[\alpha_\perp(\phi) - \alpha_i(\phi)] \tag{1}$$

Noting that the circulation of the wake vortices is $-[d\Gamma(\phi)/d\phi]\,d\phi$, one may use the Biot-Savart law to obtain[3,4]

$$\alpha_i(\phi) = \frac{1}{8\pi R u} \fint_{-\phi_0}^{\phi_0} \frac{d\Gamma(\phi')}{d\phi'} \cot \frac{\phi - \phi'}{2}\, d\phi' \tag{2}$$

Thus, for each ϕ in $(-\phi_0, \phi_0)$,

$$\frac{2\Gamma(\phi)}{u c(\phi) a(\phi)} + \frac{1}{8\pi R u} \fint_{-\phi_0}^{\phi_0} \frac{d\Gamma(\phi')}{d\phi'} \cot \frac{\phi - \phi'}{2}\, d\phi' = \alpha_\perp(\phi) \tag{3}$$

To obtain a unique solution for Γ, this equation should be supplemented by the edge conditions

$$\Gamma(-\phi_0) = \Gamma(\phi_0) = 0 \tag{4}$$

stating, on physical grounds, that no pressure differences may exist at the wingtips.

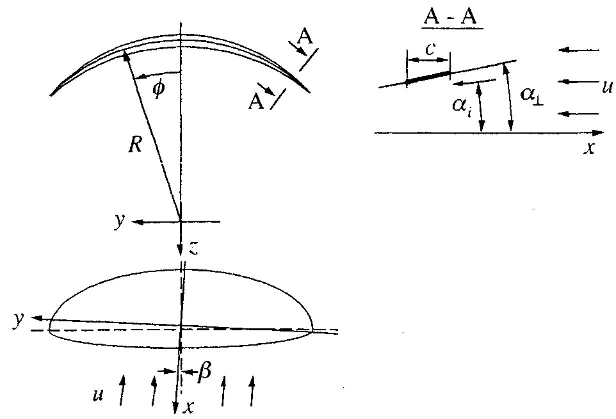

Fig. 1 Arched wing in asymmetric flight.

Equation (3) will be simplified using the substitution

$$t = \tan(\phi/2), \qquad t' = \tan(\phi'/2), \qquad t_0 = \tan(\phi_0/2) \tag{5}$$

Thus, with

$$\cot\frac{\phi - \phi'}{2} = \frac{1 + tt'}{t - t'}, \qquad \cos\phi = \frac{1 - t^2}{1 + t^2}$$
$$\sin\phi = \frac{2t}{1 + t^2}, \qquad d\phi = \frac{2\,dt}{1 + t^2} \tag{6}$$

one finds that for each t in $(-t_0, t_0)$,

$$\frac{2\bar{\Gamma}(t)}{u\bar{c}(t)\bar{a}(t)} + \frac{1}{8\pi Ru}\fint_{-t_0}^{t_0}\frac{d\bar{\Gamma}(t')}{dt'}\,\frac{1 + tt'}{t - t'}\,dt' = \bar{\alpha}_\perp(t) \tag{7}$$

Here, as well as on all subsequent occurrences, a bar accent indicates a composite function of the argument 2 arctan(·); for example,

$$\bar{\Gamma}(t) = \Gamma(2\arctan t) \tag{8}$$

The integral on the right-hand side (RHS) of Eq. (7) can be simplified further using the identity

$$1 + tt' = 1 - t(t - t') + t^2 \tag{9}$$

and the variant

$$\bar{\Gamma}(-t_0) = \bar{\Gamma}(t_0) = 0 \tag{10}$$

of Eq. (4); it yields

$$\fint_{-t_0}^{t_0}\frac{d\bar{\Gamma}(t')}{dt'}\,\frac{1 + tt'}{t - t'}\,dt' = (1 + t^2)\fint_{-t_0}^{t_0}\frac{d\bar{\Gamma}(t')}{dt'}\,\frac{dt'}{t - t'} \tag{11}$$

Thus, Eq. (3) eventually becomes: for each t in $(-t_0, t_0)$,

$$\frac{2\bar{\Gamma}(t)}{u\bar{c}(t)\bar{a}(t)} + \frac{1 + t^2}{8\pi Ru}\fint_{-t_0}^{t_0}\frac{d\bar{\Gamma}(t')}{dt'}\,\frac{dt'}{t - t'} = \bar{\alpha}_\perp(t) \tag{12}$$

Equation (12) is similar to the comparable equation from the classical lifting-line theory of straight planar wings. It suggests that an arched wing will typically produce smaller lift toward the tips than a comparable planar wing (of span $4Rt_0$) having the same chord $\bar{c}$ and AOA $\bar{\alpha}_\perp$ [note the coefficient $(1 + t^2)$ at the second term on the left-hand side of Eq. (12)]. Conversely, an arched wing with chord $\bar{c}$ and AOA $\bar{\alpha}_\perp$ will have the same lift distribution as a planar wing (of span $4Rt_0$) with chord $(1 + t^2)\bar{c}$ and AOA $\bar{\alpha}_\perp/(1 + t^2)$. Moreover, the lift distribution of an arched pseudoelliptic wing with

$$\bar{c}(t) = c_0\frac{(t_0^2 - t^2)^{1/2}}{t_0(1 + t^2)} \tag{13}$$

and $\bar{a}(t) = a_0 = \text{const}$ is governed by the same equation as that of a twisted planar elliptic wing; the latter equation is known to be solvable analytically.[1] The particular case of a pseudoelliptic wing is discussed in the remaining part of this Note.

Spanwise Lift Distribution of a Pseudoelliptic Wing

For a pseudoelliptic wing [see Eq. (13)], one may use the substitution

$$t = -t_0\cos\vartheta \tag{14}$$

to recast Eq. (12) into the form where for each ϑ in $(0, \pi)$,

$$\frac{2\bar{\Gamma}(-t_0\cos\vartheta)}{uc_0a_0\sin\vartheta} + \frac{1}{8\pi uRt_0}\fint_0^\pi\frac{d\bar{\Gamma}(-t_0\cos\vartheta')}{d\vartheta'} \times \frac{d\vartheta'}{\cos\vartheta' - \cos\vartheta} = \frac{\bar{\alpha}_\perp(-t_0\cos\vartheta)}{1 + t_0^2\cos^2\vartheta} \tag{15}$$

As in the classical lifting-line theory, a solution of this equation can be sought in the form of the Fourier series

$$\bar{\Gamma}(-t_0\cos\vartheta) = 4uRt_0\sum_{n=1}^{\infty}A_n\sin n\vartheta \tag{16}$$

where $\{A_1, A_2, \ldots\}$ is a set of constant coefficients. With Eq. (16), Eq. (15) becomes

$$\sum_{n=1}^{\infty}A_n\sin n\vartheta(1 + nH) = 2H\sin\vartheta\,\frac{\bar{\alpha}_\perp(-t_0\cos\vartheta)}{1 + t_0^2\cos^2\vartheta} \tag{17}$$

where

$$H = c_0a_0/(16Rt_0) \tag{18}$$

is a dimensionless constant. Multiplying both sides of Eq. (17), in turn, by $\sin\vartheta$, $\sin 2\vartheta, \ldots$, and integrating between 0 and π readily yields that for each m in $\{1, 2, \ldots\}$,

$$A_m = \frac{4H}{\pi(1 + mH)}\int_0^\pi\frac{\bar{\alpha}_\perp(-t_0\cos\vartheta)\sin m\vartheta\sin\vartheta}{1 + t_0^2\cos^2\vartheta}\,d\vartheta \tag{19}$$

Let α and β be the angles of attack and sideslip, measured at the midsection of the wing. Referring to Fig. 1 for a pertinent definition of β, one has that for each ϕ in $(-\phi_0, \phi_0)$

$$\alpha_\perp(\phi) = \alpha_0(\phi) + \alpha\cos\phi - \beta\sin\phi \tag{20}$$

where, by interpretation, α_0 is the local (geometric) AOA at $\alpha = \beta = 0$.

In the case where α_0 is constant on $(-\phi_0, \phi_0)$, i.e., the wing is untwisted geometrically, the integral appearing on the RHS of Eq. (19) can be computed analytically.[5] Thus, with

$$\tau = -1 + 2t_0^{-2}(\sqrt{1 + t_0^2} - 1) = -\tan^2(\phi_0/4) \tag{21}$$

one finds that for each m in $\{1, 2, \ldots\}$,

$$A_{2m-1} = \frac{2H\tau^{m-1}(1 + \tau)}{1 + (2m - 1)H}\left[\alpha_0 + \alpha(2m - 1)\frac{(1 + \tau)}{(1 - \tau)}\right] \tag{22}$$

$$A_{2m} = \frac{2Ht_0 m\tau^{m-1}(1+\tau)^3}{(1+2mH)(1-\tau)}\beta \tag{23}$$

Lift, Side-Force, Drag, and Rolling-Moment Coefficients

In the present notation, the lift, side-force, and induced-drag coefficients can be defined by

$$C_L = \frac{2R}{uS}\int_{-\phi_0}^{\phi_0}\Gamma(\phi)\cos\phi\, d\phi \tag{24}$$

$$C_y = \frac{2R}{uS}\int_{-\phi_0}^{\phi_0}\Gamma(\phi)\sin\phi\, d\phi \tag{25}$$

$$C_{di} = \frac{2R}{uS}\int_{-\phi_0}^{\phi_0}\Gamma(\phi)\alpha_i(\phi)\, d\phi \tag{26}$$

respectively, where S is an arbitrary reference area. With Eqs. (2), (5), (14), and (16), these become

$$C_L = -\frac{32\pi R^2}{S(1-\tau)}\sum_{m=1}^{\infty}A_{2m-1}\tau^m(2m-1) \tag{27}$$

$$C_y = \frac{32\pi R^2 t_0(1+\tau)}{S(1-\tau)}\sum_{m=1}^{\infty}mA_{2m}\tau^m \tag{28}$$

$$C_{di} = \frac{4\pi R^2 t_0^2}{S}\sum_{m=1}^{\infty}mA_m^2 \tag{29}$$

Now, substitute Eqs. (18), (22), and (23) in Eqs. (27–29). If S is chosen as the total wing area, namely,

$$S = R\int_{-\phi_0}^{\phi_0}c(\phi)\, d\phi = \pi R c_0 t_0\frac{1+\tau}{1-\tau} = \pi R c_0 \sin\left(\frac{\phi_0}{2}\right) \tag{30}$$

the resulting equations can be brought into the following respective forms:

$$C_L = a_0(1+\tau)^2\sum_{m=1}^{\infty}\frac{(2m-1)\tau^{2m-2}}{1+(2m-1)H} \times\left[\alpha_0 + \alpha(2m-1)\frac{(1+\tau)}{(1-\tau)}\right] \tag{31}$$

$$C_y = a_0\beta\frac{(1+\tau)^3}{1-\tau}\sum_{m=1}^{\infty}\frac{(2m)^2\tau^{2m-1}}{1+2mH} \tag{32}$$

$$C_{di} = a_0H\frac{(1+\tau)^3}{1-\tau}\sum_{m=1}^{\infty}\tau^{2m-2} \times\left\{(2m-1)\frac{[\alpha_0(1-\tau)+\alpha(2m-1)(1+\tau)]^2}{[1+(2m-1)H]^2(1+\tau)^2} - \frac{8m^3\tau\beta^2}{(1+2mH)^2}\right\} \tag{33}$$

Note that with A denoting the AR, namely

$$A = 4R^2\sin^2\phi_0/S \tag{34}$$

one has that

$$H = \frac{a_0}{\pi A}\frac{(1+\tau)^3}{(1-\tau)^3} \tag{35}$$

Since the wing is assumed to form a circular arc in the (yz) plane, pressure forces acting on the wing yield zero rolling moment about the center of the arc. For a different reference point, say, the one situated in the (xz) plane at the distance h above the center of the wing's arc, the rolling moment is, simply,

$$C_l = -C_y h/l \tag{36}$$

where l is an arbitrary reference length. With l chosen as $2R\sin\phi_0$, the span of the wing's projection of the (xy) plane, Eq. (36) yields

$$C_l = -a_0\beta\frac{h(1-\tau^2)}{4Rt_0}\sum_{m=1}^{\infty}\frac{(2m)^2\tau^{2m-1}}{1+2mH} \tag{37}$$

Approximate Formulas

For a typical gliding parachute ϕ_0 rarely exceeds 45 deg, in which case τ equals about -0.04, by Eq. (21). Accordingly, to the very good accuracy, one can neglect all terms that are of the second order (and higher) with respect to τ. This leads to the following useful approximations:

$$\frac{\partial C_L}{\partial\alpha_0} = a_0\left[\frac{1+2\tau}{1+H} + \mathcal{O}(\tau^2)\right] \tag{38}$$

$$\frac{\partial C_L}{\partial\alpha} = a_0\left[\frac{1+4\tau}{1+H} + \mathcal{O}(\tau^2)\right] \tag{39}$$

$$\frac{\partial C_y}{\partial\beta} = 4a_0\tau\left[\frac{1+4\tau}{1+2H} + \mathcal{O}(\tau^2)\right] \tag{40}$$

$$\frac{\partial C_l}{\partial\beta} = -a_0\frac{h\tau}{Rt_0}\left[\frac{1+4\tau}{1+2H} + \mathcal{O}(\tau^2)\right] \tag{41}$$

$$C_{di} = \frac{H}{a_0}(1-4\tau)\left(C_L^2 - \frac{1}{2\tau}C_y^2 + \cdots\right) = \frac{1+2\tau}{\pi A}\left(C_L^2 - \frac{1}{2\tau}C_y^2 + \cdots\right) \tag{42}$$

In Eq. (42), the ellipses stand for terms of the order $\alpha^2\tau^2$, $\alpha_0^2\tau^2$, and $\beta^2\tau^2$. Note that as far as only pressure forces are concerned, the dihedral effect of an arched wing is destabilizing relative to any point in the (xz) plane located between the wing and the center of its arc.

When A is sufficiently large and $|\tau|$ is sufficiently small, Eqs. (39) and (42) can be shown to agree with the comparable results of the asymptotic lifting-line theory developed in Ref. 3. Toward this end, it proves convenient to select the area of the wing's projection on the (xy) plane, namely,

$$S' = R\int_{-\phi_0}^{\phi_0}c(\phi)\cos\phi\, d\phi = S\frac{1+\tau^2}{(1-\tau)^2} = S[1+2\tau+\mathcal{O}(\tau^2)] \tag{43}$$

as a reference area. The corresponding AR, lift, and drag coefficients become $A' = AS/S'$, $C_L' = C_L S/S'$, and $C_{di}' = C_{di}S/S'$ by definition. Accordingly, from Eqs. (39) and (42),

$$\frac{\partial C_L'}{\partial\alpha} = a_0[(1+2\tau) - 2(1+6\tau)A'^{-1} + \cdots] \tag{44}$$

$$C_{di}' = \frac{1+2\tau}{\pi A'}\left(C_L'^2 - \frac{1}{2\tau}C_y^2 + \cdots\right) \tag{45}$$

Subject to Eq. (21) the identity between these two equations and Eqs. (44) and (45) of Ref. 3 becomes readily apparent.

References

[1]Glauert, H., *The Elements of Aerofoil and Airscrew Theory*, Cambridge Univ. Press, Cambridge, England, UK, 1983, pp. 92, 93, 137–141.

[2]Batchelor, G. K., *An Introduction to Fluid Dynamics*, Cambridge Univ. Press, Cambridge, England, UK, 1990, pp. 93, 94, 585–588.

[3]Iosilevskii, G., "Asymptotic Theory of High-Aspect-Ratio Arched Wings in Steady Incompressible Flow," *Journal of Fluid Mechanics*, Vol. 303, Nov. 1995, pp. 367–377.

[4]Belotserkovskii, S. M., *The Theory of Thin Wings in Subsonic Flow*, Plenum, New York, 1967, p. 95.

[5]Gradshteyn, I. S., and Ryzhik, I. M., *Table of Integrals, Series, and Products*, Academic, 1980, p. 369.

Wind-Tunnel Tests of Flap Gap Seals on a Two-Dimensional Wing Model

Hubert C. Smith*
Pennsylvania State University,
University Park, Pennsylvania 16802
and
John W. Schneider†
General Electric Aircraft Engines,
Cincinnati, Ohio 45215

Nomenclature

$C_{L_{max}}$ = airplane or wing lift coefficient
$C_{l_{max}}$ = section lift coefficient
$C_{l_{max_f}}$ = section lift coefficient with flaps deflected
$C_{l_{max_0}}$ = section lift coefficient with zero flaps
Re = Reynolds number based on chord length
S = wing area
S_f = area of wing segment containing flaps
α = angle of attack
δf = flap deflection angle

Introduction

A COMMERCIALLY marketed drag reduction kit was installed and flight tested on a Piper Arrow II by the first author of this Note in 1989.[1] Predominant among the devices included were gap seals for both the wing flaps and ailerons, but several fairings for flap hinges, fuel-tank-attach screws, and exposed portions of retracted wheels were also included. The primary purpose of the tests was to evaluate the effectiveness of these devices in reducing drag. Since the effect of each device was too slight to be measured individually, the entire kit was installed and tested by measuring various performance parameters. The results showed a slight reduction in parasite drag coefficient of about 18 counts, or 7% below that of the unmodified aircraft.

An unexpected result of these tests was a slight reduction in maximum lift coefficient and corresponding increase in stall speed, with the modifications installed. The change was slight, but occurred in all cases tested. The increased stall speed was about 1 or 2 mph. A senior thesis project[2] verified these results in a wind tunnel, although at very small Reynolds numbers ($Re = 1.43 \times 10^5$–1.87×10^5). This model was also three dimensional.

Flap gap seals were also investigated as part of the Advanced Technology Light Twin-Engine airplane program.[3] Although wind-tunnel tests indicated greater maximum lift with the seals in place, flight tests of the full-scale aircraft revealed the opposite. The flight tests were only performed with flaps retracted; however, the sealed flaps reduced the maximum lift coefficient by 0.19, or 5 mph higher stall speed, compared to the unsealed condition.

Although no data have been published, Mooney Aircraft Corporation tested gap seals on the Mooney TLS. Conversations with Mooney engineers indicated that a slight drag reduction was achieved, which accounted for about a 2-kn increase in cruise speed. Careful adjustment and testing was required to achieve this result, however, without altering the stall speed.

Since very little information could be found on the effects of gap seals, especially those on stall speed, it was decided to pursue further investigation. A thorough aerodynamic study of the effects of flap gap seals in a controlled environment of a wind tunnel was deemed necessary. Also, since the few previous tests that were done were primarily on three-dimensional wings, it was decided to approach this study from a two-dimensional aspect.

To compare the results with previous flight tests, the airfoil of the Piper Arrow II was used, namely a NACA 65_2-415. This airfoil was also utilized in the study of Ref. 2.

Procedure

A model was constructed for testing in the Pennsylvania State University low-speed wind tunnel, which has a test section of approximately 3.5 × 5 ft. The chord was 11.813 in., which represents a 3/16 scale of the full-size Piper Arrow. A 16-in. span was chosen, with large endplates to simulate a two-dimensional wing, which fitted into walls inserted within the tunnel.

Lift and drag forces were measured by use of an Aerolab six-component, pyramidal, strain gauge balance. Airspeed was determined by a ceiling-mounted pitot–static tube in the forward portion of the test section, which fed into a pressure transducer, and the resulting pressure differential displayed as voltage on a voltmeter. Both the balance and the pitot–static system were calibrated prior to actual testing. Tare runs were also made to determine the drag of the endplates and balance struts.

Tests were run at a speed near the highest sustainable speed of the tunnel (168 ft/s), which yielded a Re of 9×10^5. To gain some insight into Reynolds number effects, runs were also made at $Re = 6 \times 10^5$, or a speed of 112 ft/s. Since these Reynolds numbers were well below those of the full-scale airplane, a trip-strip was installed at the 30% chord position to fix the transition point. This location was chosen as a result of information in Ref. 4.

Runs were made at each of the four flap settings of the full-scale airplane: 0, 10, 25, and 40 deg. Data were taken at 14 points from −4 to +16 deg angle of attack, in 2-deg increments from −4 to +10, and 1-deg increments from 10 to 16 deg (the stall region). All tests were run with and without gap seals installed, and at both $Re = 6 \times 10^5$ and 9×10^5.

Flow visualization was performed by use of heavyweight cotton thread tufts taped to the wing. Twelve spanwise rows with seven tufts chordwise in each row were utilized, all equally spaced. Photos were made of the tuft patterns at angles of attack of 4 deg to full stall in 2-deg increments, and also 1 deg before stall. Oil flow studies were also conducted with a brightly fluorescing motor oil thinned with kerosene, and illuminated with uv lights.

Received Aug. 26, 1995; presented as Paper 95-3973 at the AIAA 1st Aircraft Engineering, Technology, and Operations Congress, Los Angeles, CA, Sept. 19–21, 1995; revision received Nov. 26, 1995; accepted for publication May 8, 1996.

*Assistant Professor, Department of Aerospace Engineering, 233 Hammond Building. Associate Fellow AIAA.

†Design Engineer, High-Speed Civil Transport Project Group.